

Toward Environmentally Friendly Photolithographic Materials: A New Class of Water-Soluble Photoresists

Shintaro Yamada,[†] Thomas Mrozek,[‡] Timo Rager,[§] Jordan Owens,[⊥] Jose Rangel, and C. Grant Willson*

Department of Chemistry and Chemical Engineering, The University of Texas at Austin, Austin, Texas 78731

Jeffery Byers[#]

International SEMATECH, Austin, Texas 78741

Received April 10, 2003; Revised Manuscript Received August 12, 2003

ABSTRACT: New water-soluble styrenic polymers bearing two functional groups, pendant ammonium salts of half-esters of malonic acids and acid-labile alkyl esters, were synthesized and evaluated for water-soluble positive-tone photoresist application. These polymers feature two solubility switches: insolubilization of the entire film by baking and selective solubilization upon exposure to UV light. Time-resolved FT-IR measurement of the baked films showed sequential evaporation of ammonia from the films and the decarboxylation of the malonate half-esters. The rates of decarboxylation depend on the structure of the substituents at the 2-position of the malonates. The choice of acid-labile esters, the structure of the half-esters, and the polymer compositions were carefully optimized, and high-resolution positive tone images were obtained that were fully processed in aqueous media.

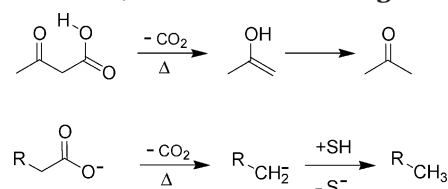
Introduction

Recent economic strategies are becoming more and more sensitive to environmental issues.¹ Efforts have been made to reduce the amount of waste organic solvent produced by the photolithographic processes. This would not only have a significantly positive impact on the environment but also reduce waste disposal costs.² Replacing the organic solvents in photoresists with water, i.e., performing the wafer coating from an aqueous solution, would greatly reduce this waste stream.

Initial approaches to design of resists for aqueous processing were based on solubility switching by either photoinduced cross-linking reaction³ or polarity change⁴ in polymers. These early systems lacked the required photosensitivity. To circumvent the sensitivity issue, our group in collaboration with professor J. M. J. Fréchet's group at University of California at Berkeley exploited the concept of a chemical amplification to develop a variety of sensitive negative tone systems using cross-linking mechanisms.⁵ Alternatively, switching mechanisms featuring polarity change were developed on the basis of ring-closure reactions of maleic acid⁶ or the pinacol rearrangement.⁷

In this paper we present the results of work on a new approach to the design of water-soluble positive tone photoresist materials.^{2,8} By definition, positive tone imaging generates solubility in exposed areas while the unexposed areas remain insoluble. All the components of the photoresist have to be water-soluble in order to cast a film from water. Therefore, two solubility switches

Scheme 1. Decarboxylation of Carboxylic Acids and Their Salts (SH = Proton-Donating Group)



had to be incorporated into the resist material, which makes the realization of the design rather challenging.

Our approach involves using the post-application bake (PAB) as the means to initially insolubilize the water-borne films and subsequent solubilization of exposed areas using acid-catalyzed chemical amplification type deprotection reactions. More specifically, the PAB not only removes casting solvent (water) from the film but also renders the film water-insoluble by inducing a chemical reaction. By incorporating a photoacid generator (PAG), acids generated only in the exposed areas catalyze another type of reaction that renders the exposed areas water-soluble. The concept of the two solubility switches has been demonstrated by our group using a cross-linking–de-cross-linking reaction of vinyl ethers.⁷ However, this system showed poor dry-etch resistance and short shelf life. We therefore sought another switching mechanism, which has more practical performance. One approach to achieving the two changes in solubility is by combining a decarboxylation of carboxylic acids and an acid-catalyzed ester cleavage. Appropriately substituted carboxylic acids can be decarboxylated either as the free acid or in the salt form.⁹ β -Keto carboxylic acids, for example, undergo thermal decarboxylation to produce the ketone and carbon dioxide, typically at temperatures below 100 °C. The mechanism is believed to involve a six-membered cyclic transition state (Scheme 1).¹⁰

It is one of a subset of carboxylic acids in which the corresponding salts decarboxylate faster than the free acids at the same temperature. For example, 2-cyano-2-(4-phenylbutanoic acid)¹¹ and phenylbis(phenylthio)-

[†] Current address: Shipley Company, 455 Forest Street, Marlborough, MA 01752.

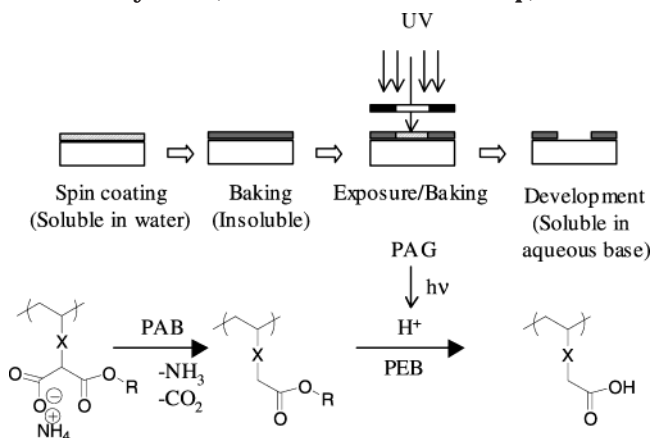
[‡] Current address: Great Lakes Manufacturing GmbH, Teplitzstr. 14-16, 84467 Waldkraiburg, Germany.

[§] Current address: MPI for Solid State Research, Heisenbergstrasse 1, 70569 Stuttgart, Germany.

[⊥] Current address: International SEMATECH, Austin, TX 78741.

[#] Current address: KLA-Tencor Texas–Finle Division, Austin, TX 78759.

* To whom correspondence should be addressed: e-mail willson@che.utexas.edu.

Scheme 2. Design Concept of the Decarboxylation System (R = Acid-Cleavable Group)

acetic acid¹² decarboxylate more slowly as the free acids than they do in the presence of amines.¹³ On the other hand, most carboxylic acids including malonic acid decarboxylate faster than their salts.¹⁴ On the basis of this knowledge, we have chosen the ammonium salt of a half-ester of malonic acid as the core unit for the two solubility switching, as illustrated in Scheme 2.

The ammonium salts of the half-esters of malonic acids provide the initial solubility for the polymer and are comparatively stable in aqueous base solutions. During the PAB, the ammonia is volatilized and the free acid decarboxylates. This decarboxylation reaction converts the acidic polymer into a neutral lipophilic species that is insoluble in aqueous base. Once the film is insolubilized, photoacid-catalyzed thermolysis of an ester, the reaction commonly used in chemically amplified resists, renders exposed areas soluble in aqueous base developer, providing positive tone images. To ensure that our new photoresist provides sufficient dry-etch resistance, a styrene backbone was chosen for this design. In the following pages, we describe the synthesis and evaluation of water-soluble polymers designed for positive tone photoresist systems that can be fully processed in aqueous media.

Experimental Section

Materials. All chemicals were purchased (Aldrich, Acros, Fluka, Merck) and used as received unless noted otherwise. Tetrahydrofuran (THF), diethyl ether, and 1,4-dioxane were refluxed over sodium benzophenone ketyl and then distilled. *tert*-Butyl alcohol was refluxed over CaH₂ and distilled. 2,2'-Azobis(isobutyronitrile) (AIBN) was recrystallized from ethanol. All the photoacid generators were obtained from Midori Kagaku Co. except triphenylsulfonium nonaflate (TPS-Nf), which was obtained from Clariant Corp. and Shipley Co. The details of the syntheses of all the monomers and polymers are described in Supporting Information.

Measurements. FT-IR spectra were collected using a Nicolet Avatar 360 IR spectrometer. Spectra of films and liquids were collected using doubly polished silicon wafers, NaCl, KBr, or KRS-5 crystal plate as substrates. KBr pellets were prepared for solid samples. ¹H and ¹³C spectra were recorded on a 300 MHz Varian Unity Plus 300 spectrometer (¹H, 300 MHz; ¹³C, 75 MHz) and were referenced to the solvent or tetramethylsilane. Mass spectra were measured on a Finnigan MAT TSQ-700 spectrometer. Gas chromatographs were recorded on a Hewlett-Packard 5890 series II with a capillary column HP-5 (cross-linked 5% phenylmethylsiloxane) and flame ionization detector. Molecular weights were measured from THF solutions using a Viscotek gel permeation chromatograph (GPC) equipped with a set of two columns (linear mix and 100 Å) from American Polymer Standards.

Table 1. Decomposition Temperature of Polyacrylates in the Presence of Triphenylsulfonium Hexafluoroantimonate¹⁵

	I)	II)	III)	IV)
T _{dec} [°C] ^a	<50	120	>200	>200
T _{dec} [°C] ^b	204	270	232	214

^a With exposure at 248 nm. ^b Without exposure at 248 nm.

Molecular weights are reported relative to polystyrene standards. Polymers containing acidic functional groups were treated with either diazomethane or trimethylsilyldiazomethane before GPC measurement. Differential scanning calorimetry (DSC) measurements and thermal gravimetric analyses (TGA) were performed by a Perkin-Elmer series 7 thermal analysis system.

Film Analysis of Polymers with FT-IR. An aqueous solution of polymers was prepared by simply mixing solid polymer (0.3 g), water (1.7 g), and ammonium hydroxide (approximately 30 wt %, 0.12 g). Polymer **6ib** gradually dissolved and a clear solution was obtained after a few hours stirring. If the polymer was not soluble in aqueous ammonia, dioxane was used instead. This solution was spin-coated on gold-coated, double-polished silicon wafers. The films were baked at various temperatures, and real-time IR spectra were collected using Nicolet Avatar 360 IR spectrometer.

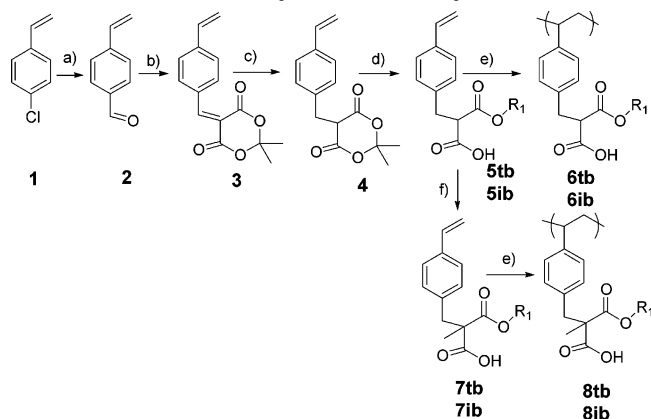
Photolithography. Preliminary evaluations were carried out using a Headway spin-coater, a JBA LS65 1 kW exposure system with a 248 nm band-pass filter from Acton Research, and an Optoline quartz mask for contact printing. The resist was projection-printed on Ultratech XLS 248 nm exposure tool (NA = 0.53; σ = 0.74) at SEMATECH or on an ASM lithography PAS 5500 248 nm stepper (NA = 0.63; σ = 0.6) at Shipley Co. The exposed films were developed with a Shipley MF CD-26 developer. Etch rates were measured on an LAM 9400 PTX tool operating at 450 W/45 W with a pressure of 20 mTorr and employing 75 sccm of Cl₂.

Results and Discussion

Choice of Acid-Labile Groups. The choice of acid-labile ester group is critical. Although half-esters of malonic acids are expected to exhibit the switching properties discussed above, i.e., thermally induced decarboxylation and subsequent acid-catalyzed deprotection of the ester, the selectivity of these two reactions is an issue. Taking into account that the esters might be accidentally cleaved via pyrolysis in the course of the PAB process, we had to find a protecting group that is thermally stable to survive the bake yet cleavable by photo acids in order to guarantee an efficient double switching function. Several polyacrylates with different ester groups were prepared, and the decomposition temperature of the polymers in the presence and absence of photogenerated acids was measured. Three secondary esters were tested in hope of providing better thermal stability compared to *tert*-butyl ester, a commonly used acid-labile functionality in commercial 248 nm photoresists. A variety of acid-labile esters were auditioned, and the results are shown in Table 1.

The cyclohexenyl (**III**) and 2-cyclohexanonyl (**IV**) acrylates decompose at higher temperatures than poly(*tert*-butyl acrylate) (**I**). They are also stable to 200 °C in the presence of photogenerated acid. Poly(isobornyl acrylate) (**II**) has a relatively low decomposition temperature in the presence of photogenerated acid but is more thermally stable than poly(*tert*-butyl acrylate). Trefonas et al. showed that the activation energy of acid-

Scheme 3. Synthesis of Vinylbenzyl-Substituted Derivatives: (a) Mg, DMF; (b) Meldrum's Acid, Piperidine, AcOH; (c) NaBH₄; (d) R₁OH, BHT (inhibitor); (e) AIBN; (f) LDA, MeI; R₁ = *tb* (*tert*-Butyl), *ib* (Isobornyl)



catalyzed deprotection of the isobornyl ester is about 2 times that of *tert*-butyl ester.¹⁶ Isobornyl esters are more thermally stable than *tert*-butyl ester under acidic conditions but are still cleavable with photoacids. From these results we conclude that both the *tert*-butyl ester and the isobornyl ester are candidates for integration as photo acid labile switching units.

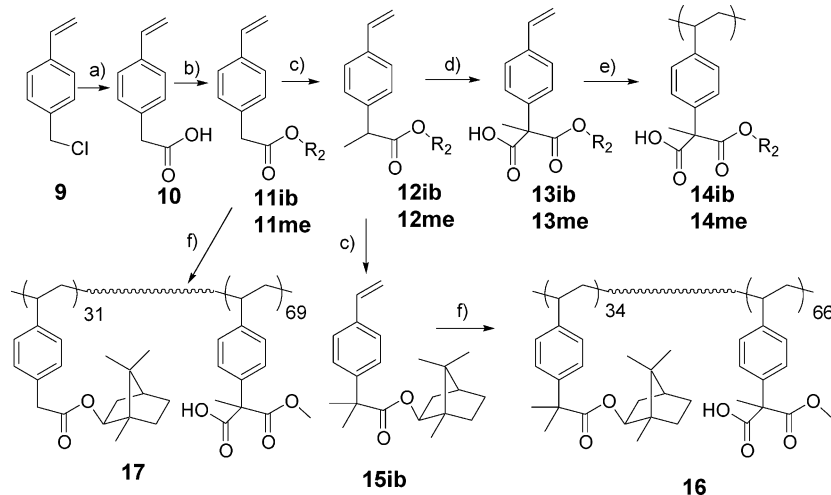
Preparation of Polymers. In the design of the synthesis of the final target polymer, we decided to choose styrenic monomers because of the relative ease of their polymerization with conventional free radical polymerization and their ability to impart dry-etch resistance in the lithographic process. The styrene unit was linked to half-esters of malonic acids in a variety of ways, as shown in Scheme 3 and Scheme 4. Three patterns of substitution at the α -position of the malonate (vinylbenzyl, vinylbenzyl + methyl, vinylphenyl + methyl) and two acid-labile groups, *tert*-butyl and isobornyl, and a methyl group were prepared for comparison. The vinylbenzyl-substituted monomers **5tb** and **5ib** were prepared from 4-chlorostyrene, **1**, in four steps. The Grignard reagent prepared from 4-chlorostyrene was reacted with *N,N*-dimethylsulfonamide (DMF) followed by hydrolysis with ammonium acetate, affording 4-vinylbenzaldehyde, **2**, in 50% yield.¹⁷ A Knövenagel condensation of this aldehyde and Meldrum's acid in the

presence of piperidine and acetic acid afforded compound **3**, which was immediately converted to the monosubstituted Meldrum's acid **4** via reduction with NaBH₄.¹⁸ No reduction of the styrenic double bond was observed. At this stage, ring opening was necessary prior to polymerization in order to circumvent gel formation.¹⁹ Refluxing **4** and the alcohol, i.e., *tert*-butyl alcohol or isoborneol in dioxane, respectively, successfully achieved this goal. In this case, the presence of added radical inhibitor 2,6-di-*tert*-butyl-4-methylphenol (BHT) was important in order to prevent oligomerization. BHT is reported to open the ring,²⁰ but an excess of alcohol and a catalytic amount of BHT gave excellent selectivity, and the desired half-esters **5tb** and **5ib** were obtained without a measurable amount of BHT adduct. Polymerization of **5tb** and **5ib** with AIBN produced the homopolymers **6tb** and **6ib**, respectively. The ammonium salts of these polymers are water-soluble. Monomer **5ib** was selectively methylated with methyl iodide using 2 equiv of lithium diisopropylamide (LDA).²¹ A simple alkylation reaction of half-esters of malonates with 4-vinylbenzyl chloride was also used to prepare these monomers. However, it required more steps and tedious purification.

The vinylphenyl-substituted monomers were prepared by modification of the reported procedure by Fréchet et al.¹³ The Grignard reaction of vinylbenzyl chloride, **9**, with carbon dioxide (50% yield) followed by esterification with isoborneol and trifluoroacetic anhydride (TFAA) afforded isobornyl (4-vinylphenyl)acetate, **11ib** (30% yield). The methyl ester, **11me**, was prepared with methyl iodide using 1,8-diazabicyclo[5.4.0]undec-7-ene (DBU) as a base (54% yield). The esters **11** were methylated with methyl iodide and LDA. Carboxylation of the resulting compounds **12** with LDA and carbon dioxide afforded monoacids **13**. Polymerization of **13** with AIBN afforded the desired homopolymer **14**. Alternatively, separation of the acid-labile group from the thermally sensitive functionality resulted in copolymerizing the isobornyl derivative **11ib** or **15ib** with monomer **13me** to give copolymers **17** and **16**, respectively. The copolymer ratios of polymer **17** and **16** were determined by ¹H NMR, and polymer **17** contains 31% of **11ib** and polymer **16** contains 34% **15ib**.

Thermal Gravimetric Analyses. TGA was used to determine the selectivity between decarboxylation and

Scheme 4. Synthesis of Vinylphenyl-Substituted Derivatives: (a) Mg, CO₂; (b) TFAA, R₂OH; (c) LDA, MeI; (d) LDA, CO₂; (e) AIBN, 13me; (f) AIBN, 13Me; R₂ = *ib* (Isobornyl), *me* (Methyl)



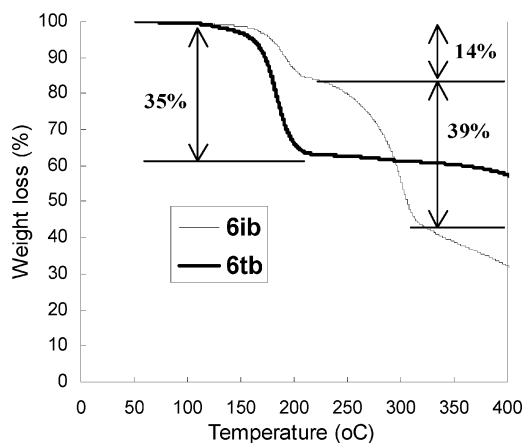


Figure 1. TGA thermograms of polymers **6tb** and **6ib**. Heating rate: 10 °C/min.

decomposition of the ester. Figure 1 shows the thermograms of polymers **6tb** and **6ib**. These polymers exhibit significantly different decomposition features. In the case of **6tb**, weight loss starts around 130 °C, and the first loss is about 35 wt %. This corresponds to the theoretical weight loss for the combined loss of CO₂ (15.9 wt %) and isobutene (20.2 wt %). Polymer **8tb** showed the same result. The selectivity between the decarboxylation of the acid group and thermolysis of the *tert*-butyl ester is not as high as we had hoped. This poor selectivity was also confirmed in a model compound study using ¹H NMR.²² The calculated loss for **6ib** is 12% for CO₂ and 39% for the protecting group. Thus, the first weight loss represents only decarboxylation, and the second weight loss is due to the loss of the protecting group. The thermogram shows a distinct division between decarboxylation and ester deprotection. The selectivity between the thermolysis of the malonic acid and isobornyl ester is quite high for this new polymer **6ib**. Other polymers bearing isobornyl and methyl groups showed the same selectivity.

Film Study with FT-IR. To more precisely analyze the decarboxylation and decomposition reactions of *tert*-butyl and isobornyl ester, respectively, an FT-IR study was carried out with spin-coated films of polymers **6tb**, **6ib**, and **8tb** cast from aqueous ammonia. Figure 2 shows the IR spectra of polymers **6tb**, **6ib**, and **8tb** undergoing baking at 165 °C. Rapid volatilization of ammonia can be observed as indicated by the disappearance of the carboxylate anion peak at ca. 1580 cm⁻¹ accompanied by the increase in the carboxylic acid carbonyl stretching band around 1715 cm⁻¹ in all three cases. The sequential decarboxylation can be observed as indicated by the decrease in the carbonyl peak intensity. Whereas primarily the high-frequency part (1743 cm⁻¹) of the carbonyl peak from **6tb** and **8tb** significantly decreases in intensity as baking time increases, a similar observation can be made only for the low-frequency part (~1714 cm⁻¹) of the same IR peak from **6ib**. The thermal behavior of the latter polymer clearly indicates that decarboxylation is the only reaction that occurs after evaporation of ammonia. In the case of **6tb** and **8tb**, decarboxylation is not the only reaction. The decrease of the peak intensity at 1743 cm⁻¹ ($\nu_{C=O}$ of ester) as baking time increases indicates that the *tert*-butyl ester is subject to concomitant decomposition. Moreover, evolution of a new peak at 1812 cm⁻¹ is observed for **6tb** but not for **8tb**. The new peak at 1812 cm⁻¹ can be assigned to $\nu_{C=O}$ of anhydride,

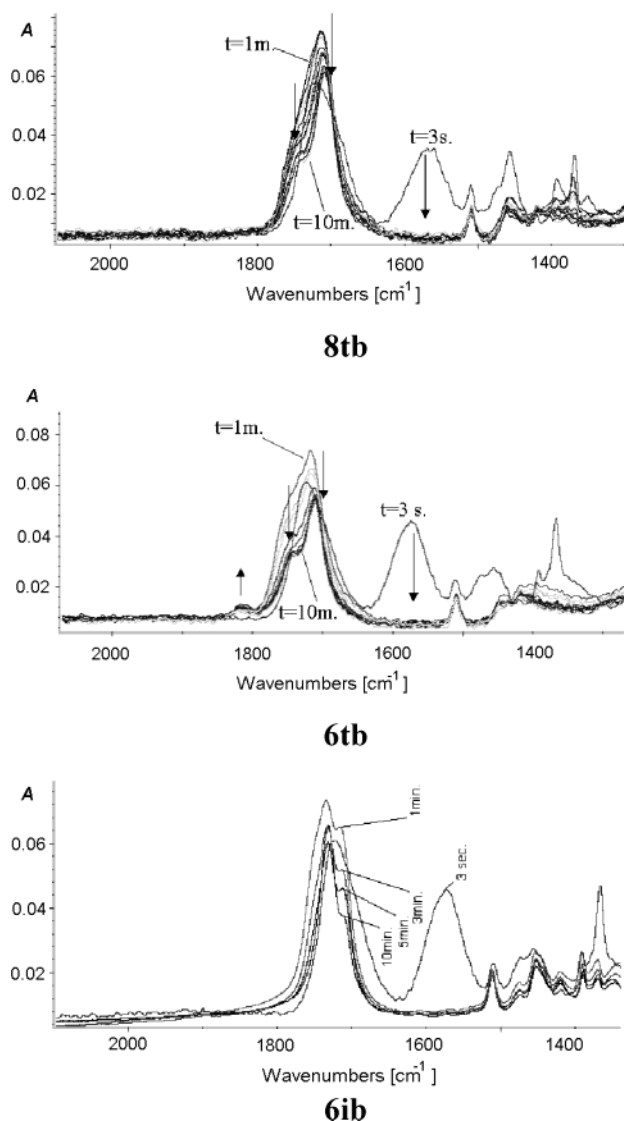


Figure 2. FT-IR spectra of ammonium salts of polymers **8tb**, **6tb**, and **6ib** after baking. Total baking time at 165 °C: 10 min.

and this indicates that some of the carboxylic acid in polymer **6tb** is subject to anhydride formation during baking. No peaks that correspond to the anhydride are observed in **8tb**, indicating that increased steric hindrance by the extra methyl group at the α -position effectively inhibits this side reaction.

A more detailed study of the release of ammonia and of the decarboxylation (Scheme 5) of **6ib** was conducted in which the polymer films were baked as before. The changes in the IR spectrum were monitored over time. Figure 3 shows the time evolution of changes in COO⁻ stretch (1628–1527 cm⁻¹). As ammonia evaporates, the COO⁻ stretch of the ammonium salt of **6ib** decreases. The ammonia evaporated within 6 s.

Figure 3 shows changes over time in the total C=O stretches of the carboxylic acid and the ester (1786–1660 cm⁻¹). As ammonia evaporates, the carboxylate turns to carboxylic acid, which has an IR peak at 1721 cm⁻¹, and this peak decreases as decarboxylation takes place. The evaporation of ammonia is much faster than the decarboxylation. Thus, a steep increase in the peak intensity is observed during the early stage of baking. The initial intensity was normalized to unity because theoretically there was only a C=O stretch of the ester

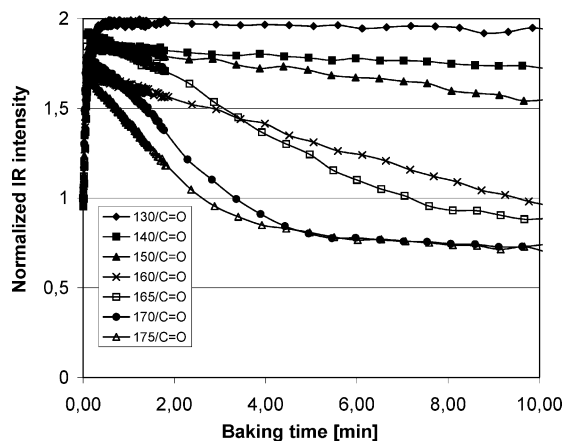
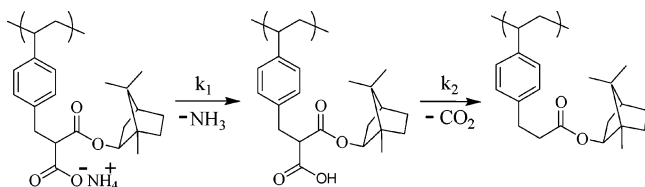


Figure 3. Time evolution of changes in C=O stretch (1786–1660 cm^{-1}) of polymer **6ib**–ammonium salt. Inset: baking temperatures in $^{\circ}\text{C}$.

Scheme 5. Transformation of Ammonium Salt of **6ib**



group before baking. As ammonia evaporates, the C=O of carboxylic acid increases, and eventually the peak intensity reaches 2 if decarboxylation reaction during the evaporation of ammonia is negligible. The peak intensity then decreases as decarboxylation takes place. The peak intensity should return to unity after decarboxylation is completed, but in fact it was less than unity. This may be due to the time lag between the spin-coating and the IR measurement, which may have resulted in some premature volatilization of ammonia that would affect the initial signal intensity.

Reaction rate constants were calculated using the IR concentration data. Although evaporation of ammonia and decarboxylation ($A \rightarrow B \rightarrow C$) are sequential reactions, the rate constants could be calculated independently because volatilization of ammonia was so much faster than decarboxylation.²³ The time evolution of the IR signal intensities for both reactions is well described by simple exponentials, as expected for first-order kinetics. Arrhenius plots were generated for the temperature-dependent rate constants (Figure 4a,b), and the activation energies of both reactions were calculated. The activation energy of ammonia volatilization is 9.2 kcal/mol, and the activation energy of decarboxylation is 39.6 kcal/mol. Wallraff et al. reported kinetics studies on thermal decomposition of poly(*tert*-butyl methacrylate).²⁴ The activation energy calculated for the thermal decomposition of poly(*tert*-butyl methacrylate) was 40.9 kcal/mol, close to that of decarboxylation. This explains the low reaction selectivity of the previous polymer bearing *tert*-butyl ester (**6tb**).

The decarboxylation kinetics of polymers **6ib**, **8ib**, **14ib**, **14me**, **16**, and **17** were studied using the same IR equipment. The ammonium salts of polymers **8ib** and **14ib** were not water-soluble; hence, all the polymers were dissolved in 1,4-dioxane. These solutions were spin-coated on gold-coated, double-polished silicon wafers. The films were baked at various temperatures, and IR spectra were collected as described previously. Figure 5 shows the time evolution of changes in C=O stretches

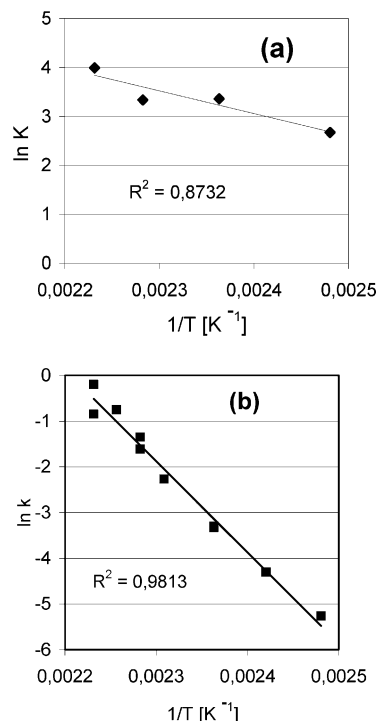


Figure 4. Arrhenius plots of **6ib**: (a) volatilization of ammonia; (b) decarboxylation.

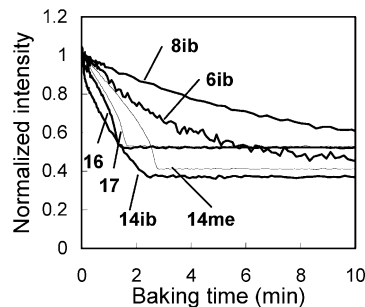


Figure 5. Time evolution of changes in C=O stretch (1786–1660 cm^{-1}) of polymers **6ib**, **8ib**, **14ib**, **14me**, **16**, and **17**.

of carboxylic acid and ester (1786–1660 cm^{-1}) for the six polymers with baking at 180 $^{\circ}\text{C}$.²⁵ IR data of the six polymers at different baking temperatures are shown in Figures 12–17 in the Supporting Information. The results are summarized in Table 2. Decarboxylation of polymers **6ib** and **8ib** followed first-order decay kinetics. No anhydride formation was observed with polymer **8ib** while **6ib** showed anhydride peak at higher baking temperature than 170 $^{\circ}\text{C}$. Interestingly, the kinetics of the thermolysis of polymers **14me**, **16**, and **17** showed autocatalytic-type behavior. The rate of decarboxylation slowly increases as baking time increases. From the mechanical point of view, the decarboxylation reaction follows first-order kinetics. However, the mechanism is apparently dependent upon the polymer structure. Various factors can affect the rate of decarboxylation, especially in a film. For example, the T_g and polarity of the polymer change drastically as decarboxylation proceeds. The polymer films are initially highly polar, and their T_g values are high. As decarboxylation takes place, the T_g and polarity decrease. If the T_g changes, the mobility of the polymer chain changes, and this could influence the reaction rates. The bulkiness of the ester group may also affect the ease of formation of the six-membered ring to induce decarboxylation. The decar-

Table 2. Comparison of Polymers 6ib, 8ib, 14ib, 14me, 16, and 17²⁶

polymer	anhydride formation ^a	order of kinetics	$T_{(de-CO_2)}^c$ at 180 °C (min)	E_a (kcal/mol)	A^e	aq sol ^f
6ib	Y	1st	8.3	29.4	5.09×10^{13}	S
8ib	N	1st	27.9	30.3	1.16×10^{15}	I
14ib	N	1st or 0	2.5	36.2 ^d	3.53×10^{17}	I
14me	N	auto ^b	2.9			S
16	N	auto ^b	1.7			S
17	N	auto ^b	1.6			S

^a Y = observed, N = not observed. ^b Autocatalytic type behavior. ^c Time for complete decarboxylation. ^d Calculated from first-order fitting. ^e Arrhenius preexponential factor. ^f Aqueous solubility: S = soluble; I = insoluble.

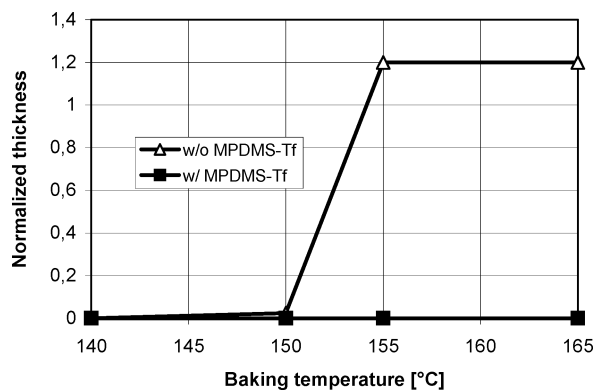


Figure 6. Change in normalized film thickness of polymer 6ib. Baking time: 5 min.

boxylation rate dramatically increased when one methylene unit was removed from polymer 8ib. Complete decarboxylation occurs 2–3 times as fast as in that of polymer 6ib.

Lithographic Evaluations. Baking Test and Evaluation of PAG. On the basis of the results of the thermal analysis and aqueous solubility of the polymers, lithographic evaluation of polymer 6ib was performed. An aqueous solution of the ammonium salt of polymer 6ib was coated on silicon wafers, and the baking temperature was varied in order to determine the threshold temperature for effective film retention toward an aqueous developer. All the films were baked for 5 min and immersed in TMAH (2.38 wt %) for 30 s for development. Figure 6 shows the normalized film thickness after development. One can see that the polymer films become insoluble in the developer when baked above 150 °C. This positive result proves that the selectivity between decarboxylation and deprotection of the isobornyl ester, as shown by the TGA and IR analysis, is sufficiently high to perform the first thermally induced solubility switch. It is also seen from Figure 6 that the film has swollen by approximately 20% after development; this phenomenon will be discussed in detail later. When the polymer was mixed with a water-soluble PAG, 4-methoxyphenyldimethylsulfonium triflate (MPDMS-Tf), there was no film retention under the same baking conditions.

Figure 7 shows the TGA thermogram of MPDMS-Tf, triphenylsulfonium triflate (TPS-Tf) and -nonaflate (TPS-Nf), which are widely used in various chemically amplified resist systems. MPDMS-Tf decomposes at lower temperatures than TPS-Nf or TPS-Tf, starting slowly around 150 °C. The thermal decomposition of the PAG generates acid, which in turn cleaves the isobornyl protecting group rendering the film soluble. This finding led us to omit MPDMS-Tf from further experimentation. TPS-Tf and TPS-Nf are both thermally stable, but TPS-Nf and TPS-Tf are not as water-soluble as MPDMS-Tf. TPS-Nf and TPS-Tf are slightly soluble in water, at least

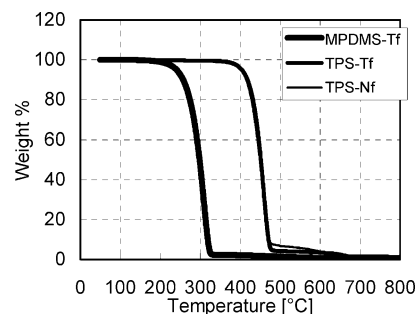


Figure 7. TGA thermogram of PAGs.

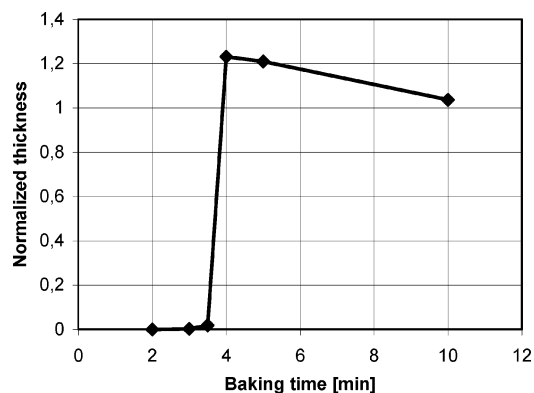


Figure 8. Change of normalized thickness of polymer 6ib with TPS-Nf; baked at 165 °C.

2.0 wt % of the PAGs based on a matrix polymer. Therefore, it was possible to dissolve the PAG in an aqueous solution of polymer 6ib. An aqueous solution of ammonium salt of polymer 6ib and TPS-Nf (1.5 wt % to polymer) was spin-coated on a silicon wafer and baked at 165 °C for 2–10 min. A dramatic change in solubility can be seen between baking times of 3.5 and 4 min (Figure 8). Decarboxylation gives a decrease in acid concentration, and the solubility threshold is around 4 min baking at 165 °C. Longer baking times minimize film swelling.

The same solution was spin-coated on a gold-coated, double-polished silicon wafer. The film was baked at 165 °C for 5 min, exposed at 248 nm, and postexposure baked at 140 °C for 1 min. Figure 9 shows FT-IR spectra of the films before exposure and after PEB. The increase in peak intensity at 3432 cm^{-1} (OH stretch) and 1710 cm^{-1} (C=O stretch of acid) and decrease in peak intensity at 2953 cm^{-1} (CH_2) and 1733 cm^{-1} (C=O stretch of ester) clearly demonstrate acid-catalyzed deprotection of the isobornyl ester.

Imaging Test. Imaging tests at SEMATECH were conducted on a photoresist sample composed of polymer 6ib, TPS-Nf (1.5 wt %), water, and ammonium hydroxide. Silicon wafers were unprimed or primed with either antireflective coat DUV-30 (60 Å thickness) or HMDS. The best adhesion was obtained with DUV-30. Baking

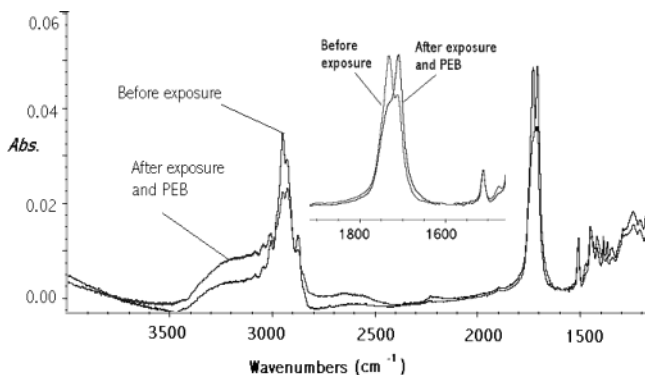


Figure 9. FT-IR spectra of polymer **6ib** with TPS-Nf before and after exposure and subsequent PEB. Exposure energy: 30 mJ/cm². Inset: spectra range from 1500 to 2000 cm⁻¹.

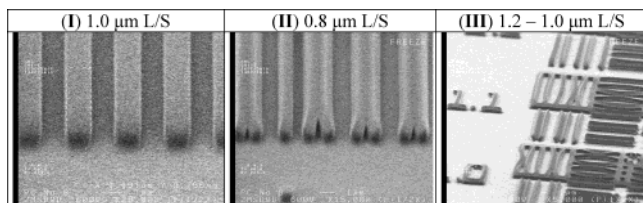


Figure 10. SEM pictures of positive tone images with polymer **6ib**. ARC: DUV 30, 61 nm; film thickness = 0.6 μm. PAB: 165 °C/5 min. Exp: 248 nm stepper. PEB: 140 °C/5 min. Developer: MF CD-26/30 s.

Table 3. Comparison of Etch Rates

	polymer 6ib	APEX-E (DUV)	SPR-510L (I-line)
etch rate (Å/min)	758	698	443
ratio	1.09	1.00	0.63

Table 4. Change of Molecular Weight by Baking

	M_n	M_w	PDI
polymer 6ib	11 800	24 600	2.09
resist film (140 °C/5 min)	11 900	27 000	2.27
resist film (165 °C/5 min)	11 400	61 500	5.40

at 165 °C for 5 min produced a 0.6 μm thick film. The insolubilized film was exposed to 248 nm radiation (20 mJ/cm²) and baked at 140 °C for 1 min. Development with Shipley MF CD-26 (TMAH 2.38 wt %) for 30 s produced 1 μm resolution positive tone images, as shown in Figure 10.

The etch rate of photoresist film containing polymer **6ib** was measured in Cl₂ plasma and compared to that of commercially available resists (Table 3). Its etch stability is not as good as the conventional I-line resist, SPR-510L, but it is comparable to the DUV resist APEX-E.

With longer baking time, e.g. 10 min, a smaller increase in thickness was observable after development (Figure 8). However, no image was obtained. This suggests the possibility of some side reactions, such as thermally induced cross-linking, during the decarboxylation process. Table 4 summarizes the change in molecular weight of the films after baking. The initial polymer **6ib** has M_w of 24 600. Baking at 140 °C induces no significant change in molecular weight. However, the GPC chromatogram showed a tailing in higher molecular weight region after baking at 165 °C for 5 min, and the resulting M_w increased significantly. The molecular weight of the film baked at 165 °C for 10 min was not measured because the film was not soluble in the GPC solvent. Although there was no anhydride peak observ-

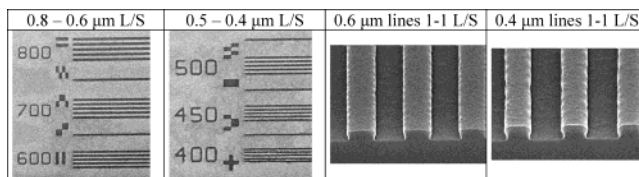
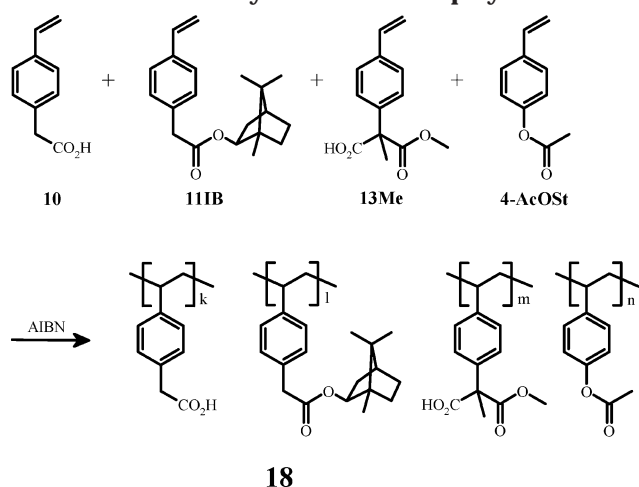


Figure 11. Top-down and cross-section SEM pictures of positive tone images of polymer **18**.

able around 1800 cm⁻¹ for **6ib** as shown in Figure 2, an anhydride peak emerged with higher baking temperature and longer baking time. Therefore, the cause of cross-linking must be the anhydride formation. Figure 2 also shows that a significant amount of carboxylic acid is left after baking for 5–10 min at 165 °C. With baking at 165 °C for 5 min, the small amount of cross-linking helped the film render insoluble in the developer. However, the small amount of cross-linking and the residual carboxylic acid caused swelling of the baked film as shown in Figures 6 and 8 and smaller features as shown in Figure 10 (III). Baking at 165 °C for 10 min produced too much cross-linking, and thus no solubility change was obtained in the exposed areas.

Optimization of Polymers. Copolymerization of two (or more) monomers with each of them being responsible for only one of the two solubility switches will offer additional variables (i.e., the comonomer ratios) for improving the imaging quality, i.e., eliminating the swelling phenomenon. Because of its fast autocatalytic decarboxylation, its high aqueous solubility and its reduced tendency for anhydride formation (Table 2), monomer **13me** seems to be particularly suited for imparting the initial solubility switching mechanism into the target copolymer without causing an observable swelling problem. Monomer **11ib**, which obviously is equivalent to monomer **15ib** when incorporated in the polymer, is supposed to represent the second solubility switch. Imaging experiments with **17** revealed that the concept of double solubility switching is transferable to copolymers. However, the decarboxylation of **17** was so fast that the resulting film after PAB became hydrophobic. Therefore, further optimization on polymer composition was conducted in order to impart the initial aqueous solubility, the two sequential solubility switches, and sufficient polarity after decarboxylation. Two additional monomers, monomer **10** and 4-acetoxystyrene (**AcOST**), were introduced into polymer **17** for this optimization (Scheme 6). The acetoxy group of **AcOST** is easily hydrolyzed by aqueous ammonia to generate phenolic groups that not only provide a moderate dissolution rate in the TMAH developer but also improve adhesion of the photoresist.²⁷ One drawback using phenolic group is that the initial solubility of the polymer in aqueous ammonia is decreased, and this narrows the options for optimizing the composition. Monomer **10** does not undergo decarboxylation and compromises this problem, but the amount should be minimized in order to avoid swelling problem as seen in Figure 10 (III). An imaging experiment with a photoresist sample composed of polymer **18** (**10/11ib/13me/AcOST** = 3/23/49/24), TPS-Nf (2.0 wt %), water, and ammonium hydroxide was conducted, and 0.4 μm resolution positive tone images were obtained, as shown in Figure 11. These results demonstrate that a photoresist based on the tetrapolymer **18** is capable of generating high-resolution images and represent an improvement of the simple homopolymer version, i.e.,

Scheme 6. Synthesis of Tetrapolymer



6ib. Further adjustments of the copolymer ratio, the formulation of the photoresist, and the process parameters, should provide even better imaging quality.

Conclusion

An aqueous processable positive tone resist material was designed using a combination of a decarboxylation reaction and an acid-catalyzed reaction of esters. This aqueous resist system possesses both high etching resistance and high resolution. The thermal stability of the ester group to decarboxylation conditions is critical for the system to function as a positive tone resist. In this regard, isobornyl esters showed stability that is superior to *tert*-butyl esters. The kinetics of the decarboxylation reaction were studied with time-resolved FT-IR, and it was found that the rate of decarboxylation is highly dependent upon substituents on the malonate moiety. Steric hindrance at the α -position played an important role to prevent anhydride formation during decarboxylation while increasing the hydrophobicity of the polymers. On the basis of these findings, we optimized a composition of tetrapolymer, and high-resolution imaging was demonstrated with DUV exposure.

Acknowledgment. We thank International SEMATECH and Shipley Co. for kindly providing us the opportunity to perform the imaging experiments at their facilities as well as the helpful assistance. Financial funding from Semiconductor Research Corp., International SEMATECH, Intel Corp., and the Welch Foundation is gratefully acknowledged. Special thanks to Prof. J. M. J. Fréchet for valuable technical discussions.

Supporting Information Available: Details of monomer and polymer syntheses and characterization. This material is available free of charge via the Internet at <http://pubs.acs.org>.

References and Notes

- (1) (a) Environmental issues caused by the "greenhouse" effect: Bradford, D. F. *Nature (London)* **2001**, *410*, 649. (b) Solvents and birth defects: Seppä, N. *Sci. News Onl.* **1999**, *155*. (c) Environmental issues in electronics manufacturing: Ellis, B. *Circuit World* **2000**, *26* (2), 17.
- (2) Yamada, S. Dissertation, The University of Texas at Austin, 2000.
- (3) Ichimura, K. *J. Polym. Sci., Part A: Polym. Chem.* **1982**, *20*, 1411.
- (4) Taylor, L. D.; Kolesinski, H. S.; Edwards, B.; Haubs, M.; Ringsdorf, H. *J. Polym. Sci., Polym. Lett.* **1988**, *26*, 177.
- (5) (a) Lin, Q.; Steinhäusler, T.; Simpson, L.; Wilder, M.; Medeiros, D. R.; Willson, C. G.; Havard, J. M.; Fréchet, J. M. J. *Chem. Mater.* **1997**, *9*, 1725. (b) Havard, J. M.; Shim, S. Y.; Fréchet, J. M. J.; Lin, Q.; Medeiros, D. R.; Willson, C. G.; Byers, J. D. *Chem. Mater.* **1999**, *11*, 719. (c) Havard, J. M.; Yoshida, M.; Pasini, D.; Vladimirov, N.; Fréchet, J. M. J.; Medeiros, D. R.; Patterson, K.; Yamada, S.; Willson, C. G.; Byers, J. D. *J. Polym. Sci., Part A* **1999**, *37*, 1225. (d) Havard, J. M.; Vladimirov, N.; Fréchet, J. M. J.; Yamada, S.; Willson, C. G.; Byers, J. D. *Macromolecules* **1999**, *32*, 86.
- (6) Darling, G. D.; Vekselman, A. M.; Yamada, S. *Proc. SPIE* **1998**, *3333*, 438.
- (7) Yamada, S.; Medeiros, D. R.; Patterson, K.; Jen, W. K.; Rager, T.; Lin, Q.; Lenci, C.; Byers, J. D.; Havard, J. M.; Pasini, D.; Fréchet, J. M. J.; Willson, C. G. *Proc. SPIE* **1998**, *3333*, 245.
- (8) Yamada, S.; Owens, J.; Rager, T.; Nielsen, M.; Byers, J. D.; Willson, C. G. *Proc. SPIE* **2000**, *3999*, 365.
- (9) March, J. In *Advanced Organic Chemistry, Reactions, Mechanisms, and Structure*, 4th ed.; John Wiley and Sons: New York, 1992; p 627.
- (10) Westheimer, F. H.; Jones, W. A. *J. Am. Chem. Soc.* **1941**, *63*, 3283.
- (11) Cram, D. J.; Haberfield, P. *J. Am. Chem. Soc.* **1961**, *83*, 2354.
- (12) Takagi, W.; Ueyama, K.; Minamida, I.; Kim, Y. H.; Ikeda, Y.; Oae, S. *Bull. Chem. Soc. Jpn.* **1966**, *39*, 917.
- (13) (a) Willson, C. G.; Cameron, J. F.; MacDonald, S. A.; Niesert, C. P.; Fréchet, J. M. J.; Leung, M. K.; Ackman, A. *Proc. SPIE* **1993**, *1926*, 354. (b) Fréchet, J. M. J.; Leung, M.; Urankar, E. J. *Chem. Mater.* **1997**, *9*, 2887.
- (14) Hall, G. A. *J. Am. Chem. Soc.* **1949**, *71*, 2691.
- (15) Polyacrylates (20 wt %) and TPS-SbF₆ (PAG, 1 wt % to polymer) were dissolved in THF. The solutions were spin-coated on silicon wafers and baked (PAB) at 100 °C for 60 s. The baked films were exposed to 248 nm light (20 mJ/cm²) and scraped off the wafers for thermal gravimetric analysis.
- (16) Trefonas, P.; Szmada, C.; Barclay, G.; Blacksmith, R.; Kavanagh, R.; Monaghan, M.; Coley, S.; Mao, Z.; Taylor, G. *Proc. Soc. Plast. Eng., Oct. 6–8, McAfee, NJ* **1997**, *11*, 44.
- (17) Dale, W. J.; Starr, L.; Strobel, C. W. *J. Org. Chem.* **1961**, *26*, 2225.
- (18) (a) Hutchins, R. O.; Rotstein, D.; Natale, N.; Fanelli, J. J. *Org. Chem.* **1976**, *41*, 3228. (b) Wright, A. D.; Haslego, M. L.; Smith, F. X. *Tetrahedron Lett.* **1979**, *25*, 2325.
- (19) The gel formation was observed only with the monosubstituted Meldrum's acid, **4**. Disubstituted Meldrum's acid (not reported here) and the opened forms (**5tb**, **5ib**) were polymerized without a gel formation. This could be due to the highly acidic α -hydrogen of Meldrum's acid ($pK_a = 4.8$). We believe that the α -hydrogen could be easily abstracted during the radical polymerization, forming a stable radical, and this radical initiated the growth of polymer chain, causing the gel formation.
- (20) Junek, H.; Ziegler, E.; Herzog, U.; Kroboth, H. *Synthesis* **1976**, 332.
- (21) (a) Ihara, M.; Takahashi, M.; Niitsuma, H.; Taniguchim, N.; Yasui, K.; Fukumoto, K. *J. Org. Chem.* **1989**, *54*, 5413. (b) Ihara, M.; Takahashi, M.; Niitsuma, H.; Taniguchim, N.; Yasui, K.; Fukumoto, K. *J. Chem. Soc. PT1* **1991**, 525.
- (22) Yamada, S.; Rager, T.; Owens, J.; Byers, J. D.; Nielsen, M.; Willson, C. G. *ACS Polym. Prepr.* **2000**, 87.
- (23) Deprotection of the ester was assumed negligible, and this was validated by TGA, IR spectroscopy, and ¹H NMR study (ref 22), all of which indicated no thermal deprotection.
- (24) Wallraff, G.; Hutchinson, J.; Hinsberg, W.; Houle, F.; Seidel, P.; Johnson, R.; Oldham, W. *J. Vac. Sci. Technol. B* **1994**, *12*, 3857.
- (25) The normalized intensity after completion of decarboxylation varies because the initial intensity contains some inherent errors. At the very early stage of baking, the casting solvent evaporates, the wafers take about 10 s to reach thermal equilibrium, and signal-to-noise ratio of spectra is much higher than that for longer baking time. These factors all affect the final intensity, and thus the final normalized intensity also changes.
- (26) Arrhenius plots of polymer **6ib**, **8ib**, and **14ib** are shown in Figure 18 in the Supporting Information.
- (27) Willson, C. G. In Thompson, L. F.; Willson, C. G., Bowden, M. J., Eds.; *Introduction to Microlithography*, 2nd ed.; American Chemical Society: Washington, DC, 1994; p 139.